

1 Lipid membranes modulate the activity of RNA through sequence-specific 2 interactions

3

4 **Authors: Tomasz Czerniak^a and James P Saenz^{a#}**

5 ^a Technische Universität Dresden, B CUBE Center for Molecular Bioengineering, 01307 Dresden,
6 Germany

7 #corresponding author and lead contact: james.saenz@tu-dresden.de

8

9 Abstract

10

11 RNA is a ubiquitous biomolecule that can serve as both catalyst and information carrier. Understanding
12 how RNA activity is controlled and how it in turn regulates bioactivity is crucial for elucidating its
13 physiological roles and potential applications in synthetic biology. Here we show that lipid membranes
14 can act as RNA organization platforms, introducing a novel mechanism for ribo-regulation. The activity
15 of R3C ribozyme can be modified by the presence of lipid membranes, with direct RNA-lipid
16 interactions dependent on RNA sequence, structure and length. In particular, the presence of guanine
17 in short RNAs is crucial for RNA-lipid interactions, while double-stranded RNAs further increase lipid-
18 binding affinity. Lastly, by artificially modifying the R3C-substrate sequence to enhance membrane
19 binding we unexpectedly generated a lipid-sensitive riboswitch. These findings introduce RNA-lipid
20 interactions as a tool for developing riboswitches and novel RNA-based lipid biosensors, and bear
21 significant implications for RNA World scenarios for the origin of life.

22

23 Introduction

24

25 RNA performs diverse functions ranging from information storage to regulation of other biomolecules
26 and direct catalysis of biochemical reactions. The functional versatility of RNA has implications for
27 understanding plausible scenarios for the origin of life¹⁻³, and for developing tools in synthetic biology⁴⁻
28 ⁶. Research aimed at understanding how an RNA World could have emerged has motivated
29 development of ribozymes with functions including RNA ligation⁷⁻¹⁰, replication^{11,12} and other
30 activities¹³⁻¹⁶. The experimental development of functional RNAs raises the possibility of RNA-based
31 synthetic systems. For both synthetic life and understanding the origin of self-replicating organisms,
32 RNA has intrinsic appeal: it can serve functions of both DNA (information storage) and proteins
33 (enzymes), obviating the need for translation machineries and protein chaperones. Furthermore, RNA
34 does not undergo irreversible denaturation like proteins, lending robustness against a broad range of
35 physical and chemical conditions. In order to design a system based on RNA, however, it is essential to
36 be able to coordinate RNA activity in space and time.

37

38 Key to harnessing the functional versatility of RNA is understanding how to spatially and temporally
39 modulate its properties and to selectively modulate the activity of different RNAs within one system.
40 The physicochemical environment surrounding an RNA molecule is a central determinant of its
41 structure, stability and activity. Spontaneous RNA hydrolysis and ligation, as well as catalytic RNA
42 activity are sensitive to pH¹⁷, ionic strength^{18,19} and RNA concentration changes¹¹, among other
43 parameters. Similarly, RNA activity can be modulated by interactions with molecules such as ions,
44 proteins, and other nucleic acids²⁰. Thus, one approach to regulating RNA activity could be via tunable

45 interactions with binding partners that affect RNA structure, concentration or chemical
46 microenvironment.

47
48 One mechanism for modulating RNA activity could be through direct RNA-lipid interactions^{19,21,22}.
49 Because of their amphiphilic nature, lipids spontaneously self-assemble into membranous structures
50 that can encapsulate RNA into protected and selective microcompartments^{23–25}. Alternatively, direct
51 RNA-lipid interactions could localize RNAs to membrane surfaces, increasing its local concentration
52 and reducing dimensionality for intermolecular interactions²¹. Lastly, localization to a lipid surface
53 brings RNA into a physicochemically unique microenvironment with sharp gradients of hydrophobicity,
54 electrical permittivity, and water activity. Through these effects, RNA-lipid interactions could provide
55 a powerful mechanism for modulating RNA activity.

56
57 The first functional RNA-lipid interaction was described more than 40 years ago²⁶, with subsequent
58 research revealing various factors that facilitate nucleic acid-lipid binding^{27–37}. More recently, specific
59 RNA sequences have been generated through SELEX with affinity for fluid membranes comprised of
60 phospholipids and cholesterol^{38–40}. Interestingly, mixtures of RNAs have also been shown to bind to
61 membranes that are in a solid crystalline (gel) phase^{41,42}. These studies revealed that, while most
62 randomized mixtures of RNA sequences can bind to gel membranes, there is a relatively small chemical
63 space of oligomers that have affinity for fluid membranes. Thus, conceptually, gel membranes could
64 provide a platform for modulating the activity of a diverse range of RNAs. However, the effects of gel
65 membranes on RNA activity and the sequence selectivity of such interactions are relatively unexplored.

66
67 This study reports the effect of lipid membranes on RNA catalytic activity. We show that RNA-lipid
68 binding depends on the primary sequence, secondary structure, and length of RNA. Using the trans-
69 acting R3C ligase ribozyme, we observed that R3C-lipid binding changes ribozyme activity in a
70 concentration-dependent manner. Lipid binding assays show that the interaction of short RNA
71 sequences with gel membranes is sequence specific and depends on guanine content and the presence
72 of double-stranded structures. Lastly, modification of R3C's substrate sequence increased the
73 tunability of R3C-based reactions through a lipid-dependent riboswitch. Our findings demonstrate that
74 membranes can serve as platforms for RNA-activity modulation, which could contribute to the
75 development of RNA-based biosensors and riboswitches. This approach introduces new tools for
76 molecular and synthetic biology and raises the prospect of previously unrecognized roles for RNA-lipid
77 interactions in the origin and evolution of life.

78

79 **Results**

80 The discovery that RNA can catalyse reactions in addition to encoding information^{18,43}, opened new
81 directions for engineering life and the possibility of protocells emerging from an RNA world². But, a
82 key missing ingredient for RNA-based systems is a mechanism to organize RNAs and regulate their
83 activity. We hypothesized that RNA-membrane interactions could influence ribozyme activity by
84 changing local RNA concentrations at the membrane surface or influencing RNA conformations.
85 Indeed, RNA oligonucleotides can bind to lipid membranes in the gel phase in the presence of divalent
86 cations, leading to aggregation into large visible RNA-lipid assemblies (**Fig. 1a**)^{27,35,41,42}. Depletion of
87 divalent cations or increasing temperature above the lipid melting temperature (i.e. producing fluid
88 instead of gel membranes) reduced RNA-membrane binding and aggregation (**Fig. 1a**). This reversible
89 aggregation could provide a tunable mechanism to concentrate and regulate RNAs in simple bottom
90 up synthetic systems, or in a prebiotic environment.

91

92 **RNA-lipid binding changes the probability of RNA-RNA interactions**

93 To determine whether local RNA concentration is influenced by interaction with lipid membranes, we
94 relied on UV-mediated crosslinking. All membranes in this study were composed of
95 dipalmitoylphosphatidylcholine (DPPC), which is in a solid crystalline (gel) phase at the experimental
96 temperature of 24°C. Nucleic acid bases absorb UV light, producing chemical changes that yield base-
97 base covalent bonds in a distance-dependent manner, yielding insights into the structure and
98 interactions of nucleic acids⁴⁴⁻⁴⁶. We first observed the effect of gel membranes on the crosslinking of
99 a single defined RNA sequence, the R3C ligase, which predominately forms one structure (R3C ligase,
100 **Fig. 1d**). When subjected to UV, the R3C ligase shows slightly increased crosslinking in the presence of
101 low lipid concentrations. A further increase in lipid concentration led to decreased crosslinking
102 efficiency, possibly through dilution of the RNA species on the surface of the lipid membranes. This
103 effect was inversely correlated with RNA-lipid binding efficiency (**Fig. 1b**). In contrast, a mixture of RNA
104 oligomers with randomized sequences which is able to create a more diverse range of intermolecular
105 structures (**Fig. 1d**) showed continuously increasing and overall higher UV-crosslinking efficiency in the
106 presence of lipids (**Fig. 1c**). The contrasting effect of crosslinking for R3C and randomized oligomers
107 might be explained by the influence of lipid membranes on RNA interactions: membrane binding could
108 potentially stabilize base-pairing⁴⁷ and thereby enhance crosslinking efficiency, whereas the decrease
109 of crosslinking might be caused by a dilution effect at higher membrane surface areas or by lipid-based
110 steric hindrance. These observations demonstrate that RNA-membrane interactions can influence
111 RNA-RNA interactions in a manner that is dependent on lipid concentration and RNA sequence
112 diversity. This further suggests that membrane binding could have an effect on trans-acting ribozyme
113 activity derived from base pairing.

114

115 **RNA-lipid interactions influence RNA catalytic activity**

116 To investigate the functional consequence of RNA-lipid binding, we tested the effect of lipids on the
117 activity of the trans-acting R3C ligase ribozyme. R3C ligase is a relatively short ribozyme that catalyzes
118 ligation of substrate strands to the ribozyme¹⁰(**Fig. 2a**). Since R3C is also part of an RNA self-replication
119 system^{11,12}, the effects of lipids on R3C are also interesting with regard to the emergence, evolution
120 and artificial synthesis of autonomous self-replicating systems. The R3C reaction rate in the absence
121 of membranes was 11 pM/min, with a reaction constant rate of $k = 6.4 \times 10^{-4} \text{ min}^{-1}$. Addition of lipid
122 vesicles led to an increased reaction rate (14 pM/min, +29%), which could plausibly be due to increased
123 ligase-substrate interaction on the membrane either through increased concentrations at the
124 membrane surface or through stabilization of base pairing⁴⁷. At the highest lipid concentration, the
125 reaction rate dropped to 8 pM/min (-27%) (**Fig. 2b**). A decrease in reaction rate was correlated with
126 further R3C ligase binding to the lipid membranes (>100 lipid/R3C, **Fig. 1b**) and we speculate that this
127 may be caused by steric hindrance from the lipid vesicles. These results show that gel membranes can
128 influence the reaction rate of a trans-acting ribozyme in a lipid concentration-dependent manner.

129

130 **R3C ligase and its substrate bind differently to the membrane**

131 To further understand how R3C and substrate membrane binding might contribute to changes in
132 ligation rates, we analyzed lipid-binding affinities of the ligase and its substrate. To quantify binding to
133 the membranes, we calculated lipid-buffer partition coefficients (K). The partition coefficient of the
134 short 12 nt substrate was more than 3 orders of magnitude lower than that of the 84 nt R3C ligase (**Fig.**
135 **2c**). Thus, in this system, substrate-membrane binding is essentially negligible compared with R3C-
136 membrane binding. Combined with our observation that RNA-RNA interactions are stabilized by

137 membrane binding (Fig. 1c), this indicates that the increased activity observed in **Figure 2b** was due to
138 an effect of the membrane on the R3C ligase-substrate complex stability, rather than through
139 substrate-lipid interactions on the membrane surface. Thus, membranes can enhance ribozyme
140 activity by promoting the stability of reaction intermediates.

141

142 **RNA sequence influences binding to gel membranes**

143 Understanding the features that influence RNA-lipid interactions could allow us to engineer RNAs with
144 higher membrane affinity, and thereby potentially enhance activity by concentrating RNAs at the
145 membrane surface. Interactions of RNA with gel-phase membranes have been previously shown to
146 exhibit low sequence-specificity, based on binding of oligos with randomized sequences^{41,42}. However,
147 the large difference in binding for R3C and its substrate suggests that RNA-gel membrane interactions
148 might in fact be dependent on RNA composition or structure.

149

150 To investigate which features of RNA influence its interaction with lipid membranes we first evaluated
151 how base content influences membrane binding of short RNA species. 19nt oligomers with only one
152 type of nucleotide were tested together with a random sequence as a control. To quantify relative
153 changes of RNA-membrane binding, we calculated the RNA binding efficiency as a percentage of total
154 RNA bound to membranes at a fixed oligo-to-lipid ratio. Remarkably, whereas the 19xG oligomer
155 bound very efficiently to the gel-phase membrane (84% binding efficiency), oligomers of A, C or U
156 showed practically no binding. A mixture of 19-mer RNA with randomized sequences showed
157 moderate binding (33% binding efficiency), as did one with AG-repeats (**Fig. 3a**), most probably due to
158 the introduction of guanine. Guanine could conceivably enhance binding either through direct
159 interactions with the membrane, or alternatively by promoting G≡C base pairing or presence of G-
160 quadruplexes, thereby influencing structure. The enhanced binding of an oligomer with only AG-
161 repeats suggests that membrane binding can be influenced by direct guanine-membrane
162 interactions⁴⁸.

163

164 We next examined the effect of deleting a specific base from mixtures of 40-mer oligos with
165 randomized sequences. Depletion of A, C or U led to a slight decrease in membrane binding, whereas
166 removal of G showed a significant binding decrease. The decrease in binding affinity in all of the base-
167 depleted oligos (**Fig. 3b**) indicates that base-pairing may influence membrane binding. However, the
168 larger effect of G depletion indicates that either depletion of G causes highest bias on RNA base-pairing
169 or base pairing is not the only factor responsible for membrane binding, consistent with our previous
170 observation that G-content alone can influence binding (Fig. 3a). Finally, by comparing 19-mer and 40-
171 mer randomized oligos, we observed that increasing RNA length also led to enhanced binding, possibly
172 due to increased length and G content (**Fig. 3 a,b**).

173

174 To further determine how guanine content affects membrane binding, lipid-buffer partition
175 coefficients were determined for short oligomers with varying G-content. RNA membrane-buffer
176 partition coefficients indicate how well a particular molecule binds to the membrane by comparing the
177 relative amount of RNA in buffer and on the lipid membrane. The RNA oligos measured in this study
178 had partition coefficients around 10^5 , which is in the range of partition coefficients determined for
179 hydrophobic peptides⁴⁹. Remarkably, addition of 2 G's per oligo led to a 2.7-fold increase of the
180 partition coefficient relative to guanine-depleted RNA. Oligos with 4 and more guanine residues
181 showed a further increase of partition coefficient values with highest value for 9 G's. This result shows

182 that the presence of guanine affects RNA-lipid binding and even low guanine content significantly
183 increases membrane binding efficiency (**Fig. 3c**).

184

185 **RNA-membrane binding is dependent on RNA structure**

186 Our observations of the effect of base depletion on oligomer binding suggested that base-pairing may
187 be a key factor in membrane binding. To investigate the effect of base-pairing-derived secondary
188 structures on membrane interactions, we estimated binding efficiency for ssRNA and dsRNA
189 (composed of 100% complementary sequences) species. We observed that not only was the
190 membrane binding efficiency higher for dsRNA compared with ssRNA species, but also that only dsRNA
191 promoted vesicle aggregation (**Fig. 4a**). It is interesting to note that the difference in binding efficiency
192 of the two ssRNAs, which have identical base composition but different sequence, is consistent with
193 the importance of sequence as a key determinant of membrane binding. We further observed that
194 dsRNA interacts with fewer lipids than ssRNA, implying different models of binding (**Fig. 4b**). Thus,
195 membrane binding efficiency can be dependent on the propensity of an RNA molecule to form intra-
196 or inter-molecular structures through base pairing.

197

198 To gain further insight into the effect of base pairing-dependent intra- and inter-molecular
199 interactions, we estimated the lipid-to-nucleotide binding ratios of ssRNA and dsRNA (**Fig. 4c**). By
200 calculating the molecular ratio of lipid/nucleotide binding, we introduce a normalization factor that
201 allows us to directly compare membrane binding for oligos of varying length. Furthermore, varying
202 lipid to nucleotide stoichiometry reflects changes in the average lipid/nucleotide interaction strength.
203 With this estimate, we compared lipid/nucleotide binding for ssRNA and dsRNA alongside oligos with
204 varying guanine content from our previous analysis (**Fig. 3c**). The differences between ssRNA and
205 dsRNA, all containing 9 guanines per oligo, confirmed our previous observation that sequence variation
206 (with constant base content) and base pairing can both influence binding. However, the reason for a
207 change in lipid/nucleotide ratio for oligos with varying guanine content was not readily apparent.
208 Analysis of oligos with varying guanine content by native non-denaturing gel revealed that the
209 presence of guanine promotes a larger spread in migration (**Fig. 4c, inset**), indicating that guanines
210 promote intermolecular interactions. These observations show that guanine can enhance binding by
211 promoting intermolecular interactions, and further confirm the importance of base pairing in RNA-
212 lipid interactions.

213

214 **Modifying R3C substrate sequence enhances membrane binding and modifies reaction rates**

215 In previous experiments, we observed that the binding affinity of the short substrate was >3 orders of
216 magnitude lower than for the R3C ligase and that reaction rates correlated strongly with R3C-
217 membrane binding (**Fig. 2c, d**). We therefore reasoned that by modifying the R3C ligase substrate to
218 enhance membrane binding, we might be able to further modulate ligase activity through increased
219 RNA density at the membrane surface. Having determined that guanine content is a key factor
220 influencing RNA-lipid binding (**Fig. 3**), we modified the R3C substrate sequence to increase lipid
221 membrane binding efficiency by addition of a 5'-overhang with varying amounts of AG repeats (**Fig.**
222 **5a**).

223

224 We first assessed the effect of modifying the R3C ligase substrate on ligation rate in the absence of
225 membranes (**Fig. 5a**). We observed that increasing the guanine content decreased ligase activity,
226 suggesting that 5' modification of the substrate was inhibiting the reaction either through steric
227 hindrance or promotion of inhibitory inter- or intra-molecular interactions. To determine whether AG-

228 rich substrates form intra-molecular structures⁵⁰ or exhibit reduced binding with the R3C ligase, we
229 performed electrophoresis in native conditions with and without ligase (**Fig. 5b**). Firstly, the non-
230 modified short substrate migrated as one band and was fully bound to the R3C ligase. Secondly, a
231 4x(AG) 20 nt substrate variant migrated as two bands, which suggests that part of the substrate
232 molecules have some folding that might bias binding to the R3C ligase. In the presence of ligase, 30%
233 of the substrate was non-bound, which correlated with a 22% reduction in reaction rate. For the
234 longest substrate variant (31 nt), electrophoretic mobility suggested higher folding, since only one
235 band was present and migrated half-way between the non-folded 12 nt and 20 nt substrates. 70% of
236 the 9x(AG) substrate was not bound to the ligase, which correlates with a reduced R3C reaction rate.
237 Lastly, the AG-rich oligomer did not co-migrate with the R3C ligase, indicating that the inhibition effect
238 is not based on non-specific substrate-ligase interactions (not shown). Therefore, increasing guanine
239 content reduces R3C ligase-substrate binding, likely accounting for decreased activity.

240
241 We next investigated whether varying guanine content through 5' modification of the substrate
242 influences membrane binding and, consequently, ligation activity in the presence of membranes. As
243 expected, the longer guanine-containing R3C substrates showed significantly higher membrane
244 binding compared with the shorter variant (**Fig. 5c**). To determine whether binding of the substrates
245 to the membrane enhances ligase activity, we determined R3C reaction rates in the presence of the
246 gel lipid membranes (**Fig. 5d**). For modified substrates, the reaction rates increased significantly to the
247 level of the unmodified substrate. Interestingly, none of the modified substrates exhibited higher
248 activity than the unmodified substrate, indicating that the rescue of activity of the other guanine
249 variants is not due to increased substrate-ligase interactions through enhanced binding to the
250 membrane, but rather due to interaction of the membrane with 5' overhangs. Thus, substrate-
251 membrane interaction increases activity by rescuing the inhibitory effect of the guanine-rich 5'
252 overhangs (**Fig. 5e**).

253
254 In summary, by modifying the R3C ribozyme substrate with an additional short sequence containing
255 guanine residues, we increased membrane affinity. The addition of guanines, however, also introduced
256 an inhibitory effect on ligation activity that was reversed through the introduction of gel-membranes
257 to the reaction. Thus, we unexpectedly produced a lipid-sensitive riboswitch-like system that could be
258 tuned in a lipid concentration-dependent manner.

259 260 **Discussion**

261
262 We have demonstrated that RNA-gel membrane interactions are dependent on the primary sequence
263 and secondary structure of ribonucleic acids. Varying the guanosine content of RNAs changed
264 membrane-buffer partitioning by several orders of magnitude. Additionally, double-stranded RNAs
265 exhibited higher membrane partitioning than single-stranded RNAs, indicating that secondary
266 structure is a critical factor in RNA-membrane interactions. Although gel-membranes are not widely
267 observed in living cells, RNA-gel membrane interactions could be employed for ribo-regulation in
268 synthetic biological systems. Gel membranes also plausibly accumulated in ancient prebiotic scenarios,
269 potentially serving as an organizational scaffold, as has been proposed for “ribofilms” on mineral
270 surfaces⁵¹. Furthermore, understanding the factors involved in RNA-gel membrane interactions should
271 provide insights that can be used to design RNA sequences with affinity for physiologically relevant
272 fluid membranes. Indeed, our finding that guanosine is a key factor in promoting RNA-gel membrane

273 partitioning is consistent with previous speculation that guanosine residues might play a role in the
274 binding of RNA aptamers to fluid membranes³⁸. Taken together, the sequence and structural
275 dependence of RNA-gel membrane interactions shown here provides the necessary framework to
276 design synthetic RNAs with varying membrane affinities.

277
278 Our observation of riboswitch-like behavior suggests a novel mechanism for regulation of RNA through
279 membrane interactions. Riboswitches are RNAs with regulatory effects that are derived from
280 sensitivity to physicochemical conditions or through binding with an interaction partner. Riboswitch
281 regulation through temperature changes, interaction with nucleic acids and small molecules have been
282 described previously^{52–56}. However, lipid sensitive riboswitches have not been documented. It is now
283 plausible that spontaneously self-assembling lipid membranes in ancient environments could have
284 served as an organizational scaffold regulating the activity of RNAs in a sequence- and structure-
285 dependent manner. Furthermore, the importance of guanosine in membrane binding suggests a
286 possible mechanism for its selection as one of the canonical nucleic acids. In extant organisms,
287 synthetic or naturally occurring RNAs exhibiting sensitivity to lipids could potentially act as biosensors
288 or riboswitches. By demonstrating that RNA-gel membrane interactions can induce riboswitch-like
289 behaviors, we raise the possibility that such functionalities could be an ancient mechanism of ribo-
290 regulation and may be present among the myriad uncharacterized small RNAs in modern cells.

291
292 RNA-membrane interactions provide a means to select RNAs by sequence and structure. For example,
293 diverse RNA species can be segregated or co-localized based on their differential membrane affinities.
294 Furthermore, selective RNA-membrane localization can be controlled by shifting the temperature
295 above and below the membrane gel-liquid transition temperature, thereby turning on and off RNA-
296 membrane binding. Such lipid-dependent sorting of RNAs could provide a mechanism to selectively
297 control the concentration of reactants in primordial scenarios and in synthetic RNA-based systems.
298 Selective RNA-membrane interactions would also influence the sequence space explored by evolving
299 ribozymes. Ribozymes generated through natural or artificial selection in the presence of lipid
300 membranes may, therefore, evolve enhanced or novel functions. The sequence and structural
301 selectivity of RNAs for membranes can also be implemented in the design of novel RNA membrane
302 biosensors. Looking forward, RNA-membrane interactions can provide tools for selective ribo-
303 regulation in synthetic systems, development of membrane biosensors, and might facilitate the
304 emergence of novel functions through artificial and natural evolution of ribozymes in the presence of
305 membranes.

306
307 In conclusion, our findings reveal that lipids, which are present in every modern cell and were plausibly
308 part of a prebiotic world^{57–59}, can interact with RNA and change its activity. These findings have
309 significant applications in fields such as synthetic biology, where merging the selective affinities of
310 aptamers with ribozyme activity (aptazymes) is currently a developing field^{60–62}. Our results provide a
311 foundation for exploring the basis of membrane-RNA interactions with physiologically relevant fluid
312 membranes exhibited by synthetic aptamers^{16,40,63} thereby providing new regulatory mechanisms in
313 synthetic biology through the specific and anchor-free localization of RNA molecules within lipid
314 compartments. Furthermore, insights from the present study can already be implemented in
315 bioengineering applications such as in improving mRNA drug delivery mechanisms and introducing
316 lipid sensitive ribo-regulation to synthetic ribozyme networks. Finally, the interaction between RNA
317 and lipid membranes could have provided an evolutionary pressure in ancient times through selection
318 for base composition or secondary structural features.

319
320

321 **Acknowledgements:**

322 We would like to thank Mario Mörl, Ilya Levental, Robert Ernst, Andre Nadler, Dora Tang, Grzegorz
323 Chwastek, Michał Grzybek and Mike Thompson for helpful discussions and feedback. This work was
324 supported by the B CUBE of the TU Dresden, a Simons Foundation Fellowship (to J.S.), a German
325 Federal Ministry of Education and Research BMBF grant (to J.S., project 03Z22EN12), and a VW
326 Foundation “Life” grant (to J.S., project 93090).

327
328 The authors declare no conflict of interests.

329

330 **References**

331

332 1. Pace, N. R. & Marsh, T. L. RNA catalysis and the origin of life. *Origins Life Evol B* **16**, 97–116
333 (1985).

334 2. Gilbert, W. Origin of life: The RNA world. *Nature* **319**, 618–618 (1986).

335 3. Rich, A. On the problems of evolution and biochemical information transfer. *Horizons in*
336 *biochemistry* 103–126 (1962).

337 4. Breaker, R. R. Engineered allosteric ribozymes as biosensor components. *Curr Opin Biotech*
338 **13**, 31–39 (2002).

339 5. Wittmann, A. & Suess, B. Engineered riboswitches: Expanding researchers’ toolbox with
340 synthetic RNA regulators. *Febs Lett* **586**, 2076–2083 (2012).

341 6. Isaacs, F. J., Dwyer, D. J. & Collins, J. J. RNA synthetic biology. *Nat Biotechnol* **24**, 545–554
342 (2006).

343 7. Bartel, D. & Szostak, J. Isolation of new ribozymes from a large pool of random sequences.
344 *Science* **261**, 1411–1418 (1993).

345 8. Eklund, E., Szostak, J. & Bartel, D. Structurally complex and highly active RNA ligases
346 derived from random RNA sequences. *Science* **269**, 364–370 (1995).

347 9. Robertson, M. P., Hesselberth, J. R. & Ellington, A. D. Optimization and optimality of a
348 short ribozyme ligase that joins non-Watson–Crick base pairings. *Rna* **7**, 513–523 (2001).

349 10. Rogers, J. & Joyce, G. F. The effect of cytidine on the structure and function of an RNA
350 ligase ribozyme. *Rna* **7**, 395–404 (2001).

351 11. Paul, N. & Joyce, G. F. A self-replicating ligase ribozyme. *Proc National Acad Sci* **99**,
352 12733–12740 (2002).

353 12. Lincoln, T. A. & Joyce, G. F. Self-Sustained Replication of an RNA Enzyme. *Science* **323**,
354 1229–1232 (2009).

- 355 13. Saragliadis, A., Krajewski, S. S., Rehm, C., Narberhaus, F. & Hartig, J. S. Thermozymes:
356 synthetic RNA thermometers based on ribozyme activity. *Rna Biol* **10**, 1009–1016 (2013).
- 357 14. Ferretti, A. C. & Joyce, G. F. Kinetic Properties of an RNA Enzyme That Undergoes Self-
358 Sustained Exponential Amplification. *Biochemistry-us* **52**, 1227–1235 (2013).
- 359 15. Lam, B. J. & Joyce, G. F. Autocatalytic aptazymes enable ligand-dependent exponential
360 amplification of RNA. *Nat Biotechnol* **27**, 288–292 (2009).
- 361 16. Janas, T., Janas, T. & Yarus, M. A membrane transporter for tryptophan composed of
362 RNA. *Rna* **10**, 1541–1549 (2004).
- 363 17. Pino, S., Ciciriello, F., Costanzo, G. & Mauro, E. D. Nonenzymatic RNA Ligation in Water*.
364 *J Biol Chem* **283**, 36494–36503 (2008).
- 365 18. Guerrier-Takada, C., Gardiner, K., Marsh, T., Pace, N. & Altman, S. The RNA moiety of
366 ribonuclease P is the catalytic subunit of the enzyme. *Cell* **35**, 849–857 (1983).
- 367 19. Anella, F. & Danelon, C. Prebiotic Factors Influencing the Activity of a Ligase Ribozyme.
368 *Life* **7**, 17 (2017).
- 369 20. Dai, X., Zhang, S. & Zaleta-Rivera, K. RNA: interactions drive functionalities. *Mol Biol Rep*
370 **47**, 1413–1434 (2020).
- 371 21. Müller, U. F. & Bartel, D. P. Improved polymerase ribozyme efficiency on hydrophobic
372 assemblies. *Rna* **14**, 552–562 (2008).
- 373 22. Anella, F. & Danelon, C. Reconciling Ligase Ribozyme Activity with Fatty Acid Vesicle
374 Stability. *Life* **4**, 929–943 (2014).
- 375 23. Chen, I. A., Salehi-Ashtiani, K. & Szostak, J. W. RNA Catalysis in Model Protocell Vesicles. *J*
376 *Am Chem Soc* **127**, 13213–13219 (2005).
- 377 24. Mansy, S. S., Schrum, J. P., Krishnamurthy, M., Tobé, S., Treco, D. A. & Szostak, J. W.
378 Template-directed synthesis of a genetic polymer in a model protocell. *Nature* **454**, 122–125
379 (2008).
- 380 25. Bianconi, G., Zhao, K., Chen, I. A. & Nowak, M. A. Selection for Replicases in Protocells.
381 *Plos Comput Biol* **9**, e1003051 (2013).
- 382 26. Budker, V. G., Kazatchkov, Yu. A. & Naumova, L. P. Polynucleotides adsorb on
383 mitochondrial and model lipid membranes in the presence of bivalent cations. *Febs Lett* **95**,
384 143–146 (1978).
- 385 27. McManus, J. J., Rädler, J. O. & Dawson, K. A. Does Calcium Turn a Zwitterionic Lipid
386 Cationic? *J Phys Chem B* **107**, 9869–9875 (2003).

- 387 28. Kharakoz, D. P., Khusainova, R. S., Gorelov, A. V. & Dawson, K. A. Stoichiometry of
388 dipalmitoylphosphatidylcholine-DNA interaction in the presence of Ca²⁺: a temperature-
389 scanning ultrasonic study. *Febs Lett* **446**, 27–29 (1999).
- 390 29. Gromelski, S. & Brezesinski, G. Adsorption of DNA to zwitterionic DMPE monolayers
391 mediated by magnesium ions. *Phys Chem Chem Phys* **6**, 5551–5556 (2004).
- 392 30. Uhríková, D., Hanulová, M., Funari, S. S., Khusainova, R. S., Šeršeň, F. & Balgavý, P. The
393 structure of DNA–DOPC aggregates formed in presence of calcium and magnesium ions: A
394 small-angle synchrotron X-ray diffraction study. *Biochimica Et Biophysica Acta Bba -*
395 *Biomembr* **1713**, 15–28 (2005).
- 396 31. Gromelski, S. & Brezesinski, G. DNA Condensation and Interaction with Zwitterionic
397 Phospholipids Mediated by Divalent Cations. *Langmuir* **22**, 6293–6301 (2006).
- 398 32. McLoughlin, D., Dias, R., Lindman, B., Cardenas, M., Nylander, T., Dawson, K., Miguel, M.
399 & Langevin, D. Surface Complexation of DNA with Insoluble Monolayers. Influence of
400 Divalent Counterions. *Langmuir* **21**, 1900–1907 (2005).
- 401 33. Michanek, A., Yanez, M., Wacklin, H., Hughes, A., Nylander, T. & Sparr, E. RNA and DNA
402 Association to Zwitterionic and Charged Monolayers at the Air–Liquid Interface. *Langmuir*
403 **28**, 9621–9633 (2012).
- 404 34. Michanek, A., Kristen, N., Höök, F., Nylander, T. & Sparr, E. RNA and DNA interactions
405 with zwitterionic and charged lipid membranes — A DSC and QCM-D study. *Biochimica Et*
406 *Biophysica Acta Bba - Biomembr* **1798**, 829–838 (2010).
- 407 35. Marty, R., N’soukpoé-Kossi, C. N., Charbonneau, D. M., Kreplak, L. & Tajmir-Riahi, H.-A.
408 Structural characterization of cationic lipid–tRNA complexes. *Nucleic Acids Res* **37**, 5197–
409 5207 (2009).
- 410 36. Suga, K., Tanabe, T., Tomita, H., Shimanouchi, T. & Umakoshi, H. Conformational change
411 of single-stranded RNAs induced by liposome binding. *Nucleic Acids Res* **39**, 8891–8900
412 (2011).
- 413 37. Lu, D. & Rhodes, D. G. Binding of phosphorothioate oligonucleotides to zwitterionic
414 liposomes. *Biochimica Et Biophysica Acta Bba - Biomembr* **1563**, 45–52 (2002).
- 415 38. Khvorova, A., Kwak, Y.-G., Tamkun, M., Majerfeld, I. & Yarus, M. RNAs that bind and
416 change the permeability of phospholipid membranes. *Proc National Acad Sci* **96**, 10649–
417 10654 (1999).
- 418 39. Vlassov, A. & Yarus, M. Interaction of RNA with Phospholipid Membranes. *Mol Biol+* **36**,
419 389–393 (2002).
- 420 40. Vlassov, A., Khvorova, A. & Yarus, M. Binding and disruption of phospholipid bilayers by
421 supramolecular RNA complexes. *Proc National Acad Sci* **98**, 7706–7711 (2001).

- 422 41. Janas, T., Janas, T. & Yarus, M. Specific RNA binding to ordered phospholipid bilayers.
423 *Nucleic Acids Res* **34**, 2128–2136 (2006).
- 424 42. Pannwitt, S., Slama, K., Depoix, F., Helm, M. & Schneider, D. Against Expectations:
425 Unassisted RNA Adsorption onto Negatively Charged Lipid Bilayers. *Langmuir* **35**, 14704–
426 14711 (2019).
- 427 43. Kruger, K., Grabowski, P. J., Zaug, A. J., Sands, J., Gottschling, D. E. & Cech, T. R. Self-
428 splicing RNA: Autoexcision and autocyclization of the ribosomal RNA intervening sequence
429 of tetrahymena. *Cell* **31**, 147–157 (1982).
- 430 44. Quarless, S. A. & Cantor, C. R. Analysis of RNA structure by ultraviolet crosslinking and
431 denaturation gel electrophoresis. *Anal Biochem* **147**, 296–300 (1985).
- 432 45. Behlen, L. S., Sampson, J. R. & Uhlenbeck, O. C. An ultraviolet light-induced crosslink in
433 yeast tRNA phe. *Nucleic Acids Res* **20**, 4055–4059 (1992).
- 434 46. Nejedlý, K., Kittner, R., Pospíšilová, Š. & Kypr, J. Crosslinking of the complementary
435 strands of DNA by UV light: dependence on the oligonucleotide composition of the UV
436 irradiated DNA. *Biochimica Et Biophysica Acta Bba - Gene Struct Expr* **1517**, 365–375 (2001).
- 437 47. Lengyel, A., Uhríková, D., Klacsová, M. & Balgavý, P. DNA condensation and its thermal
438 stability influenced by phospholipid bilayer and divalent cations. *Colloids Surfaces B*
439 *Biointerfaces* **86**, 212–217 (2011).
- 440 48. Black, R. A., Blosser, M. C., Stottrup, B. L., Tavakley, R., Deamer, D. W. & Keller, S. L.
441 Nucleobases bind to and stabilize aggregates of a prebiotic amphiphile, providing a viable
442 mechanism for the emergence of protocells. *Proc National Acad Sci* **110**, 13272–13276
443 (2013).
- 444 49. White, S. H., Wimley, W. C., Ladokhin, A. S. & Hristova, K. [4] Protein folding in
445 membranes: Determining energetics of peptide-bilayer interactions. *Methods Enzymol* **295**,
446 62–87 (1998).
- 447 50. Lee, J. S., Evans, D. H. & Morgan, A. R. Polypurine DNAs and RNAs form secondary
448 structures which may be tetra-stranded. *Nucleic Acids Res* **8**, 4305–4320 (1980).
- 449 51. Baross, J. A. & Martin, W. F. The Ribofilm as a Concept for Life's Origins. *Cell* **162**, 13–15
450 (2015).
- 451 52. Johansson, J., Mandin, P., Renzoni, A., Chiaruttini, C., Springer, M. & Cossart, P. An RNA
452 Thermosensor Controls Expression of Virulence Genes in *Listeria monocytogenes*. *Cell* **110**,
453 551–561 (2002).
- 454 53. Winkler, W., Nahvi, A. & Breaker, R. R. Thiamine derivatives bind messenger RNAs
455 directly to regulate bacterial gene expression. *Nature* **419**, 952–956 (2002).

- 456 54. Morita, M. T., Tanaka, Y., Kodama, T. S., Kyogoku, Y., Yanagi, H. & Yura, T. Translational
457 induction of heat shock transcription factor ζ 32: evidence for a built-in RNA thermosensor.
458 *Gene Dev* **13**, 655–665 (1999).
- 459 55. Schilling, O., Langbein, I., Müller, M., Schmalisch, M. H. & Stülke, J. A protein-dependent
460 riboswitch controlling ptsGHI operon expression in *Bacillus subtilis*: RNA structure rather
461 than sequence provides interaction specificity. *Nucleic Acids Res* **32**, 2853–2864 (2004).
- 462 56. Nahvi, A., Sudarsan, N., Ebert, M. S., Zou, X., Brown, K. L. & Breaker, R. R. Genetic Control
463 by a Metabolite Binding mRNA. *Chem Biol* **9**, 1043–1049 (2002).
- 464 57. Patel, B. H., Percivalle, C., Ritson, D. J., Duffy, C. D. & Sutherland, J. D. Common origins of
465 RNA, protein and lipid precursors in a cyanosulfidic protometabolism. *Nat Chem* **7**, 301–307
466 (2015).
- 467 58. Rushdi, A. I. & Simoneit, B. R. T. Lipid Formation by Aqueous Fischer-Tropsch-Type
468 Synthesis over a Temperature Range of 100 to 400 °C. *Origins Life Evol B* **31**, 103–118 (2001).
- 469 59. Brady, R. C. & Pettit, R. Mechanism of the Fischer-Tropsch reaction. The chain
470 propagation step. *J Am Chem Soc* **103**, 1287–1289 (1981).
- 471 60. Robertson, M. P. & Ellington, A. D. Design and optimization of effector-activated
472 ribozyme ligases. *Nucleic Acids Res* **28**, 1751–1759 (2000).
- 473 61. Debiais, M., Lelievre, A., Smietana, M. & Müller, S. Splitting aptamers and nucleic acid
474 enzymes for the development of advanced biosensors. *Nucleic Acids Res* **48**, 3400–3422
475 (2020).
- 476 62. Stifel, J., Spöring, M. & Hartig, J. S. Expanding the toolbox of synthetic riboswitches with
477 guanine-dependent aptazymes. *Synthetic Biology* **4**, ysy022- (2019).
- 478 63. Janas, T. & Yarus, M. Visualization of membrane RNAs. *Rna* **9**, 1353–1361 (2003).
- 479 64. Walker, S. C., Avis, J. M. & Conn, G. L. General plasmids for producing RNA in vitro
480 transcripts with homogeneous ends. *Nucleic Acids Res* **31**, e82–e82 (2003).
- 481 65. Chen, P. S., Toribara, T. Y. & Warner, H. Microdetermination of Phosphorus. *Anal Chem*
482 **28**, 1756–1758 (1956).
- 483
484
485
486
487
488
489

507

508 **B** – C, G or U

509 **D** – A, G or U

510 **H** – A, C or U

511 **V** – A, C or G

512

513 **Methods**

514 All of the RNA incubations were prepared in DNA low bind tubes (Sarstedt, Germany) at the constant
515 temperature of 24 °C in buffer comprised of 10 mM HEPES pH 7, 5 mM CaCl₂, and 5 mM MgCl₂. RNA
516 concentration was determined by measuring absorbance at 260 nm (SPARK 20M, TECAN). Before every
517 incubation RNA was preheated in SafeLock tubes (90 °C, 5 minutes; Eppendorf, Germany) to ensure
518 unfolded structures. Denaturing PAGE analysis was performed using 10% 19:1
519 acrylamide:bisacrylamide gel composition, whereas native gels were composed of 8-10% 20:1
520 acrylamide:bisacrylamide mix. Before application on the denaturing PAGE all of the samples were
521 ethanol precipitated.

522

523 Structure of R3C ligase from Fig. 1d was generated using RNA structure Fold tool from Mathews lab
524 (<https://rna.urmc.rochester.edu/RNAstructureWeb/>).

525

526 **Lipid preparation**

527 DPPC chloroform stock was pipetted into a glass vial and briefly evaporated under a steady flow of
528 nitrogen gas. To remove organic solvent residues, a lipid film was dried under vacuum overnight. To
529 obtain multi-layer DPPC vesicles (MLV DPPC), lipid films were hydrated in reaction buffer, with a final
530 lipid concentration of 10 mM in 1 mL. Buffer-lipid mixtures were shaken at 60 °C, above the melting
531 temperature of DPPC ($T_m = 42$ °C), for one hour. A cloudy liposome suspension was freeze-and-thawed
532 10x and extruded 17x through 100 nm polycarbonate filters (Merck Millipore, USA) to reduce multi-
533 lamellarity and achieve a consistent size distribution of vesicles. Lipid vesicle stocks were kept at 4 °C.
534 Stock lipid concentrations were confirmed using a phosphate assay⁶⁵.

535

536 **Dynamic light scattering**

537 The size distribution of DPPC vesicles was estimated using a ZetaSizer Nano in 173° backscatter with
538 multiple narrow mode (high resolution) analysis. Final concentration of lipids was 10 μM and the
539 amount of RNA was fixed at a ratio of 10 lipids / nucleotide. Results were plotted as the size distribution
540 in the number of detected species (NumberPSD).

541

542 **UV-crosslinking**

543 RNA was incubated for 10 minutes in the reaction buffer with or without lipids followed by 10 minutes
544 incubation under UV-B light (300 mW LEUVA77N50KKU00 LED 305 nm) from a distance of 1.5 – 2 cm.
545 Samples were analysed on denaturing PAGE with SybrGold poststaining.

546

547 **R3C activity assays**

548 5 pmol of R3C ligase was mixed with 0.5 pmol of the substrate to ensure saturation of the system
549 (pseudo 1st order reaction) and decrease any batch-to-batch differences coming from R3C purification.
550 Final reaction volume was adjusted to 30 μl. Incubation was conducted at various concentrations of
551 DPPC vesicles and samples were ethanol precipitated after 30, 60, 90 and 120 minutes. Reactions were

552 quantified on denaturing PAGE using FIJI software. Product and substrate intensities (I_P and I_S ,
553 respectively) were quantified and the concentration of product at time t was calculated:

554

$$555 \quad [P]_t = [S]_0 * \left(\frac{I_P}{I_P + I_S} \right)$$

556

557 To determine reaction rates (M/min), concentration of the product was plotted as a function of time
558 and then fitted with a linear function (fixed [0;0] point).

559

560 RNA-lipid binding assays

561 Binding assays for the results in Fig. 2c (R3C ligase), Fig. 3a, b, c and Fig. 4a were conducted using
562 liposome-coated magnetic beads. Binding assays for the results in Fig. 1b, c and 4b, c were conducted
563 using an ultracentrifugation method.

564

565 Magnetic beads binding assay

566 Magnetic beads (DynaBeads streptavidin T1, Invitrogen) were coupled with DPPC liposomes doped
567 with 0.5 mol% biotinoyl cap PE. Lipid concentration on non-diluted beads was estimated using a
568 phosphate assay⁶⁵. Liposome conjugated beads final working concentration was of 800 μ M lipid.

569

570 25 pmol of 19 nt or 10 pmol of 40/36 nt RNAs were incubated with 2 – 1.5x diluted magnetic beads for
571 30'. After incubation the supernatant was separated from the beads using a magnet. The amount of
572 RNA left in solution was estimated either using absorbance or Qubit miRNA quantification kit
573 (ThermoScientific, USA). The reported binding efficiencies (Fig. 3a, b) correspond to 15 μ L of liposome-
574 coated beads in a 30 μ L reaction volume. The partition coefficient K (Fig. 3c, Fig. 4a) was calculated
575 according to following formula:

576

$$577 \quad K = \frac{\frac{[R_L]}{[R_L] + [L]}}{\frac{[R_w]}{[R_w] + [W]}} \quad \text{Eq. 1}$$

579

580

581

582

583

584

585

586

587

588

589

590

591

592

593

594

595

Assuming high excess of [L] and [W] we simplified the equation to:

$$K = \frac{\frac{[R_L]}{[L]}}{\frac{[R_w]}{[W]}} \quad \text{Eq. 2}$$

Where:

[R_L] – RNA bound to the membranes

[R_w] – non-bound RNA

[L] – outer lipid concentration

[W] – water concentration

Ultracentrifugation binding assay

596 RNA was incubated with various concentrations of DPPC vesicles for 30'. After incubation
597 ultracentrifugation was conducted to separate vesicles from the solution (125 000 x G, 40', 24 °C). 9
598 µL of supernatant (out of 30 µL reaction mix) was pulled and incubated with 1.5 µL of 0.5 M EDTA (90
599 °C, 5'). After incubation 150 µL of 1xQubit dye was added to the solution and the amount of RNA was
600 measured using a plate reader (SPARK 20M, TECAN).

601
602 Measured fluorescence intensity values were plotted as a function of lipid/oligomer or lipid/nucleotide
603 ratios (we assumed that RNA interacts only with the outer membrane leaflet, so final outer lipid
604 concentration is equal half of the total lipid amount) and fitted using Hill's fit (OriginLab software):
605

606
$$f(x) = Start + (End - Start) \frac{x^n}{x^n + k^n} \quad \text{Eq. 3}$$

607
608 Where Start and End are function plateau values, k is inflection point of curve and n is cooperativity
609 index. Inflection point of the curve (k) is a parameter which we used for further data analysis.

610

611 **RNA-lipid binding partition coefficient determination for R3C substrates**

612 5 pmol of RNA was incubated with an excess of DPPC vesicles (5 mM, 2.5 mM outer leaflet) for 30
613 minutes. After incubation ultracentrifugation was conducted to separate vesicles from solution (125
614 000 x G, 40', 24 °C). 10 µL out of 30 µL was taken as a supernatant sample, and the rest of the
615 supernatant was discarded to leave only the pellet. RNA from supernatant and pellet samples was
616 ethanol precipitated and analyzed using denaturing PAGE. Partition coefficient values (Fig. 2c
617 "substrate", Fig. 5c) were calculated using Eq. 2.

618

619

620

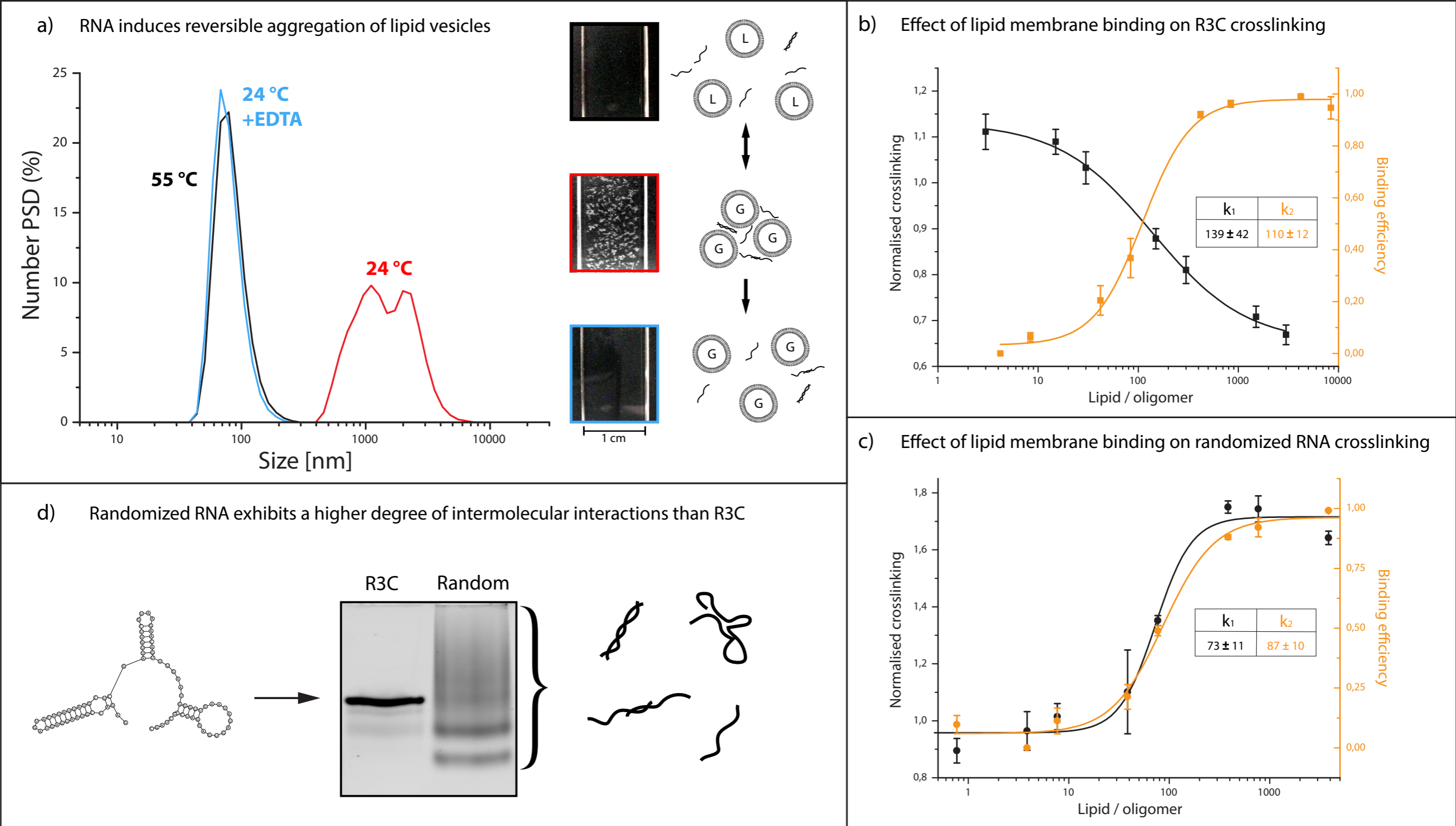
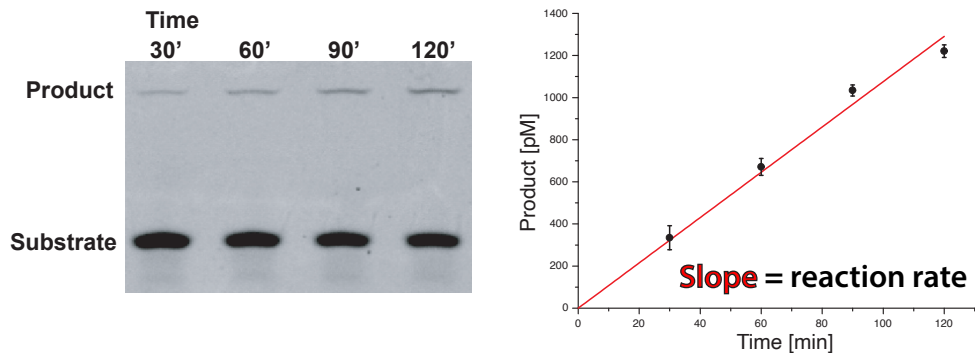
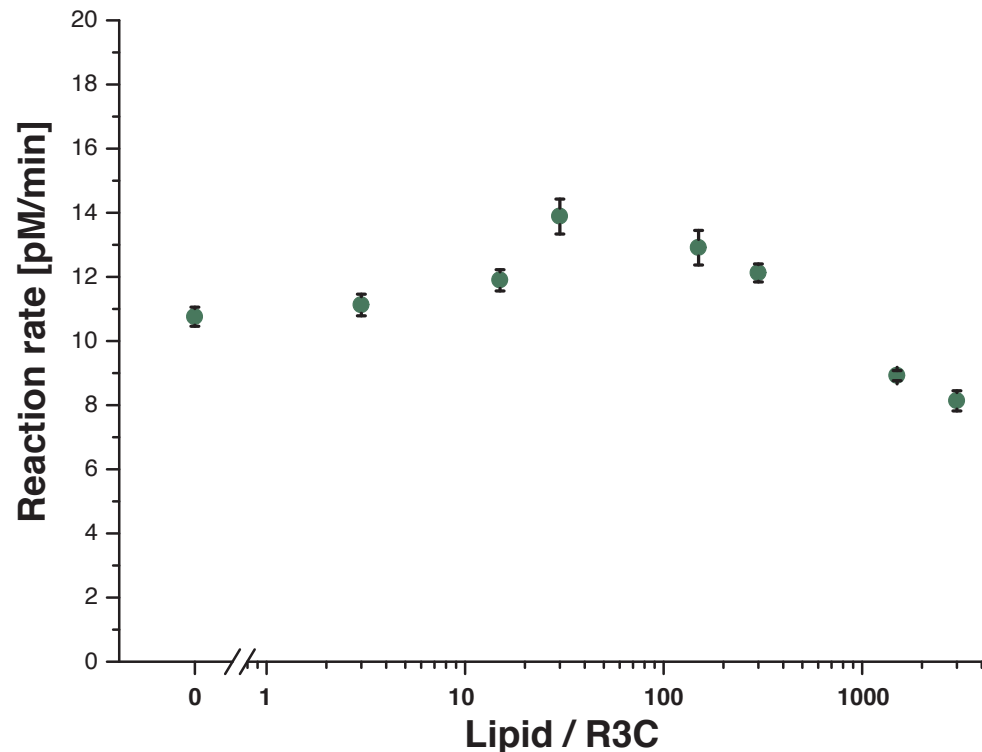


Fig. 1 RNA-lipid interactions induce reversible aggregation of vesicles and enhance intermolecular RNA interactions. (a) RNA-induced vesicular aggregation can be observed through changes in vesicle size distribution measured by dynamic light scattering (left), or visually as depicted in the cuvette images (right). The introduction of a randomized pool of RNA oligos to gel lipid membranes (gel phase = **G**) induces vesicle aggregation, which can be reversed either through chelation of divalent cations with EDTA or by increasing the temperature to achieve membranes in a liquid phase (liquid phase = **L**). **(b)** R3C ligase (84 nt) shows a small increase in UV-crosslinking at low lipid concentration, whereas crosslinking efficiency decreases at higher lipid concentration. Binding and UV crosslinking are inversely correlated and show similar inflection points with respect to lipid concentration. **(c)** Randomized RNA oligos (75-85 nt) show increasing crosslinking efficiency in the presence of lipids with a slight decrease at the highest lipid concentration; crosslinking and lipid binding are closely correlated. **(d)** Analysis of RNAs by native PAGE gel demonstrates that the R3C ligase forms primarily one structure, whereas randomized RNA forms diverse intermolecular complexes.

a) Determination of R3C ligase activity**b) Effect of lipid vesicles on R3C ligase activity****c) Lipid binding and nucleotide characteristics of R3C reactants**

Oligo	log(K)	Nucleotide %				Length
		G	A	C	U	
R3C	7.22 ± 0.08	27	28	13	31	84 nt
Substrate	3.39 ± 0.15	8	33	33	25	12 nt

Fig. 2 Lipid membranes influence R3C ligase activity through lipid-ligase interactions. (a) R3C ligase reaction rates were quantified by measuring the amount of product within a 2 hour incubation time. (b) R3C reaction rate is dependent on the presence of gel membranes - increased activity is observed for lower lipid concentration followed by drop in activity at higher lipid concentration. (c) The 12 nt R3C substrate shows several orders of magnitude lower membrane-buffer partition coefficient $\log(K)$ compared with the R3C ligase, which could be derived from different compositional or structural characteristics of both RNA species.

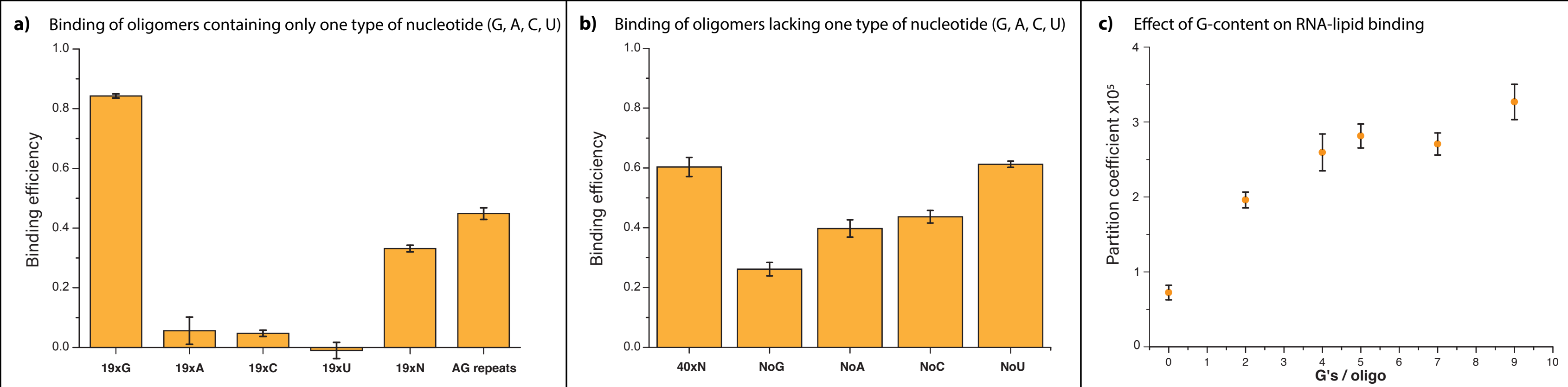
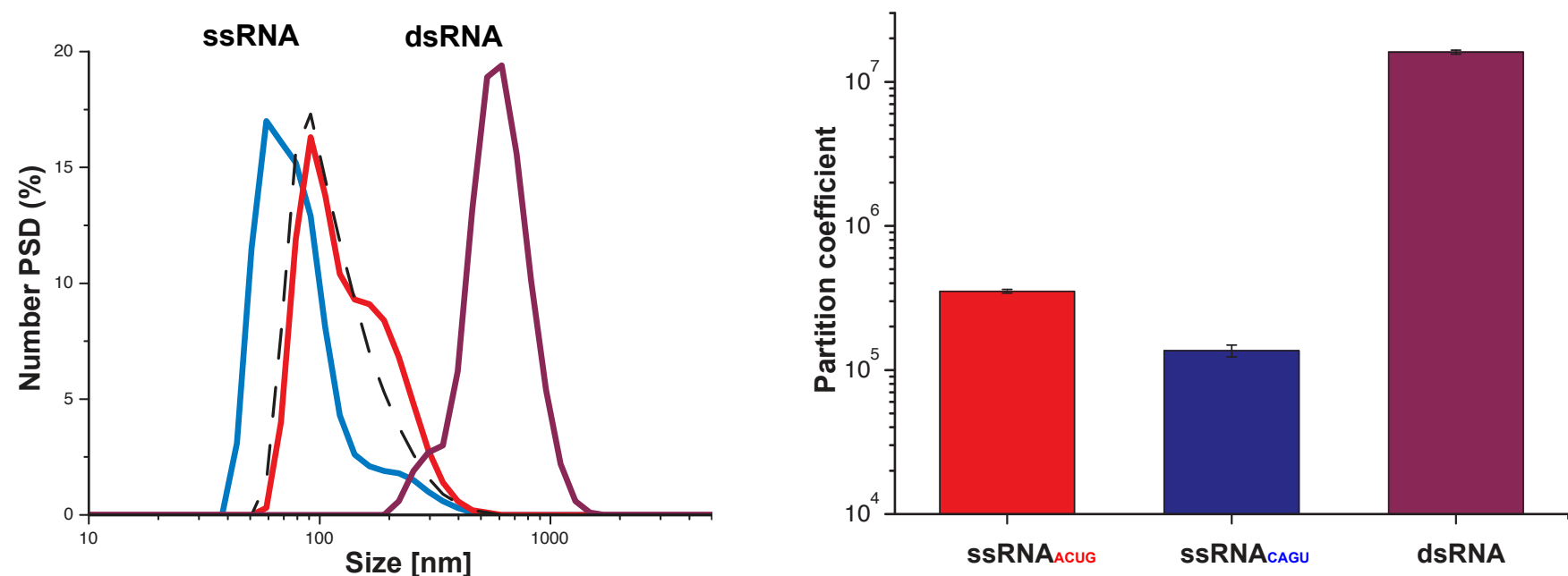
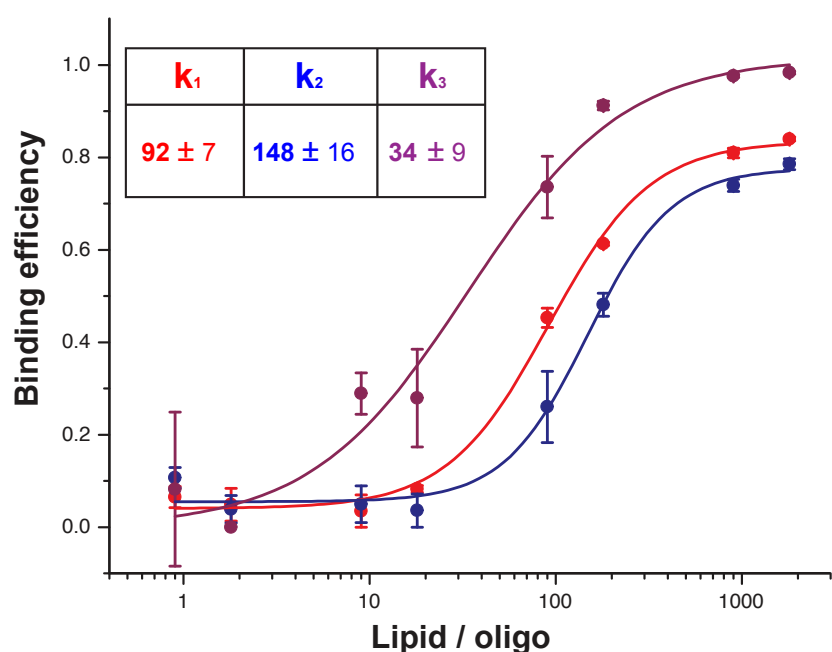


Fig. 3 RNA-lipid binding is RNA sequence-dependent. (a) Short 19 nucleotide oligomers show sequence-dependent binding to the gel membranes, with highest binding observed for the pure G oligomer followed by oligos with randomized sequence or AG repeats. Oligomers containing only A, C or U bases show negligible binding to the lipid membranes. (b) Oligonucleotide length also influences binding efficiency as seen in the comparison of (a) 19xN and (b) 40xN. Depletion of one type of nucleotide within oligomers lowers binding efficiency. Lack of guanine decreased binding by 57%, whereas lack of adenine, uracil or cytidine showed a less pronounced effect. (c) Oligonucleotides with increasing G content showed higher lipid – buffer partition coefficients compared to a G-deficient oligo with the highest value observed for the 9xG oligomer.

a) Effect of RNA base-pairing on vesicle aggregation and lipid membrane binding



b) Lipid:RNA binding ratios for ssRNA and dsRNA



c) Effect of G-content on lipid:nucleotide binding ratio

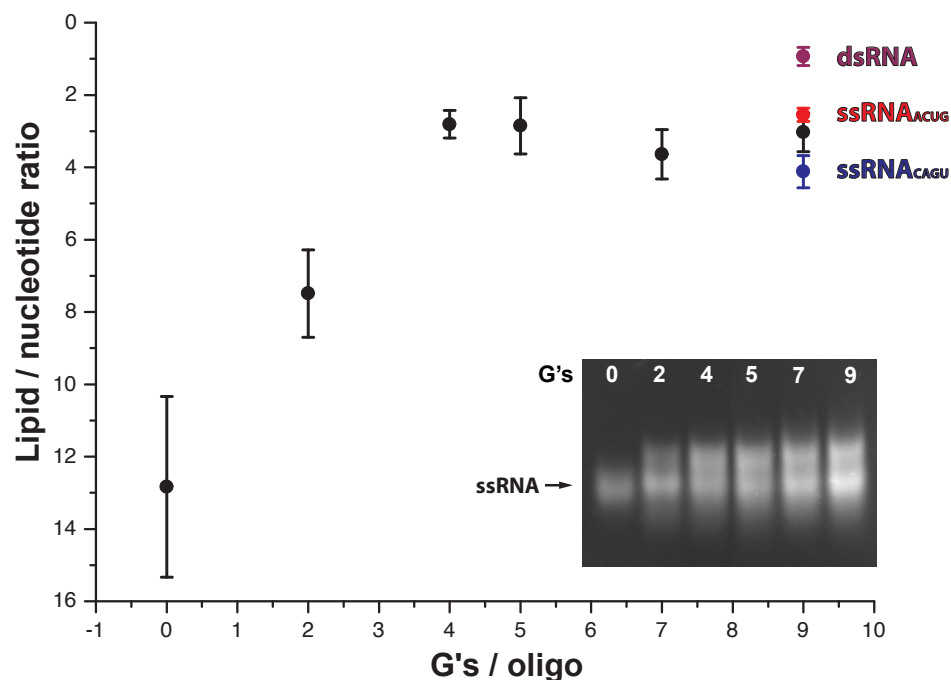


Fig. 4 RNA-gel membrane binding depends on RNA structure. (a) The effect of RNA base-pairing structure on lipid vesicle aggregation (left) and membrane binding (right) was evaluated by comparing RNA's with limited ability to create inter- and intramolecular structures (ssRNA: 36 nucleotide ACUG or CAGU repeats) with 100% complementary double stranded RNAs (dsRNA: mixed ACUG and CAGU oligos). Single stranded RNAs do not cause lipid vesicle aggregation despite moderate membrane binding, whereas double stranded RNA species show both high binding and vesicle aggregation. **(b)** RNA:lipid binding ratios (shown in table) estimated from binding curves of ssRNA and dsRNA (plotted) are affected by base pairing and sequence. **(c)** Oligomers with different nucleotide composition show different lipid/nucleotide binding stoichiometry. Analysis of oligomers by native PAGE gel (**c, inset**) indicates that the presence of guanine promotes inter-molecular interactions, suggesting, that base-pairing enhances the average strength of nucleotide-lipid interactions.

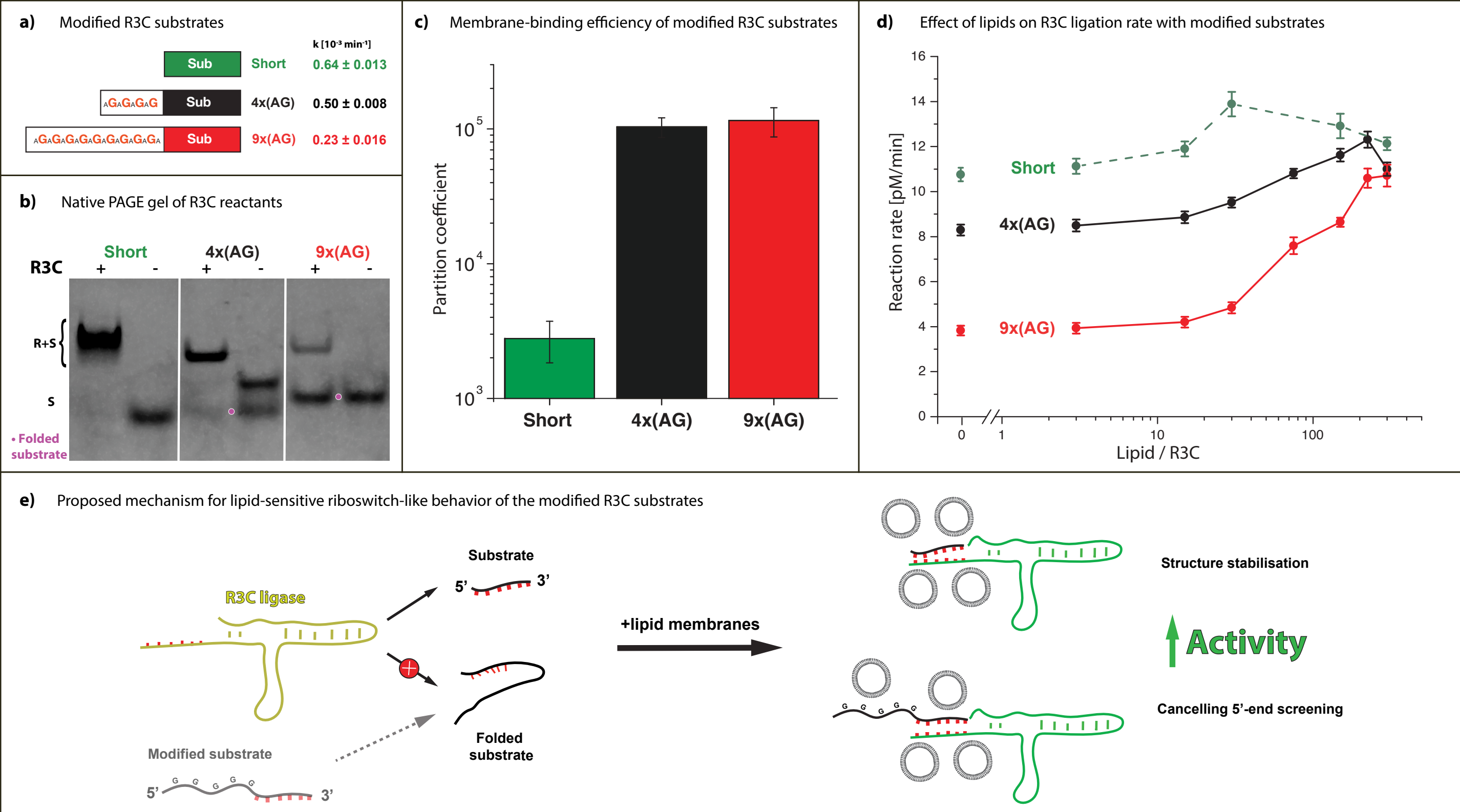


Fig. 5 **Modification of the R3C substrate sequences enables lipid-dependent tunability of ligation rate.** **(a)** Modified R3C reaction substrates were synthesized in order to increase binding to the membrane. The catalytic 3' end of the molecule was enriched with 5' tails with varying G content. Reactions for modified substrates showed lower reaction rate constants compared with the unmodified substrate. **(b)** The mechanism for inhibition of activity was evaluated by analysis of R3C reactants using native PAGE. The unmodified short substrate is entirely bound to the ligase, whereas AG-modified substrates show mobility abnormalities, which suggest substrate folding (magenta points). **(c)** Modification of the substrate sequence through addition of a 5' overhang increases binding to the membrane. **(d)** Addition of lipid membranes to reactions with the G-rich substrates increases reaction rates to the level of the unmodified substrate. **(e)** We propose that the decrease of R3C reaction rates in the presence of G-rich substrates is based on the inhibition of the catalytic part of the substrate by the 5' G-rich overhang. The presence of lipid membranes not only increases R3C-substrate stability, but also screens the 5' rich substrate part enabling the R3C reaction to proceed.